Identification of MEDIATOR16 as the Arabidopsis COBRA suppressor, MONGOOSE1

Nadav Sorek[*,1,2,3], Heidi J. Szemenyei[1,2,3], Hagit Sorek[1], Abigail A. Landers[1], Heather Knight[4], Stefan Bauer[1], David E. Wemmer[5] and Chris R. Somerville[1,2,]

[1] Energy Biosciences Institute, University of California, Berkeley CA 94720

[2] Plant and Microbial Biology Department, University of California, Berkeley CA 94720

[3] These authors contributed equally to this work

[4] School of Biological and Biomedical Sciences, Durham University, Durham DH1 3LE, UK

[5] Department of Chemistry, University of California, Berkeley CA 94720

* Correspondence: nadavsorek@berkeley.edu

Key words: Cell wall, cellulose, freezing tolerance, pectin, pectin esterification

Abstract

We performed a screen for genetic suppressors of *cobra*, an Arabidopsis mutant with defects in cellulose formation, and an increased ratio of unesterified/esterified pectin. We identified a suppressor named *mongoose1 (mon1*), that suppressed the growth defects of *cobra,* partially restored cellulose levels, and restored the esterification ratio of pectin to wild-type levels. *mon1* was mapped to the *MEDIATOR16* locus , a tail mediator subunit, also known as *SENSITIVE TO FREEZING 6* (*sfr6*). When separated from the *cobra* mutation, mutations in *MED16* caused resistance to cellulose biosynthesis inhibitors, consistent with their ability to suppress the *cobra* cellulose deficiency. Transcriptome analysis revealed that a number of cell wall genes are mis-regulated by *med16* mutations. Two of these genes encode pectin methylesterase inhibitors, which, when ectopically expressed, partially suppressed the *cobra* phenotype. This work suggests that cellulose biosynthesis can be affected by the esterification levels of pectin, either through monitoring cell wall integrity or through changing the affinity of pectin to cellulose.

Significance Statement

The *cobra* mutants of Arabidopsis, such as *cob-6*, have impaired growth associated with a defect in cellulose synthesis. Mutations in *MED16* reduce the number of misregulated genes in *cob-6* mutants and suppress the phenotypes. This observation implicates *MED16* in transcriptional responses to cell wall defects. Ectopic expression of two pectin methylesterase inhibitors (PMEIs) identified in a suppressor screen partially suppressed the growth defect in the *cob-6* mutant. The results confirm that the PMEIs have significant in vivo activity and provide evidence that pectin esterification can modulate cell wall properties.

Introduction

Cellulose, the backbone of the primary plant cell wall, supports a complex polysaccharide-rich network formed of hemicelluloses and pectin (1). Unlike other cell wall polymers, cellulose is synthesized at the plasma membrane by the cellulose synthase complex, which synthesizes multiple β−1,4 glucan chains that hydrogen-bond to form cellulose fibrils (2-5). The proposed catalytic components of the cellulose synthase complex in higher plants are the CESA proteins. However, tThe stoichiometry of the cellulose synthase complex, as well as the exact number of glucan chains in individual cellulose fibrils is unclear (3, 6-7). Additional proteins involved in some aspect of the cellulose formation process have been implicated by analysis of transcriptional networks (8-9). The Arabidopsis *COBRA* gene was found to be involved in cell expansion (10), and has been proposed to participate in cellulose synthesis (11-12). COBRA was recently shown to localize in the plasma membrane and to bind individual β−1,4 glucan chains, suggesting a role in glucan crystallization during cellulose biosynthesis (12).

During cellulose biosynthesis, other cell wall components can potentially affect the formation of fibrils by interacting with the nascent glucan chains or microfibrils. For example, in an Arabidopsis mutant that lacks xyloglucan, thicker cellulose fibrils have been observed (13), supporting the idea that xyloglucan prevents cellulose microfibril aggregation (14). Primary cell walls are also rich in pectin, which can bind cellulose with similar affinity to xyloglucan (15) and, in Arabidopsis primary cell walls, up to 50% of the cellulose is in direct contact with pectin (16). Thus, it may be anticipated that mutations that affected the structure or amount of pectin and other non-cellulosic polysaccharides may impact cell wall assembly.

The factors that regulates cell wall composition are gradually being revealed (17). Several NAC transcription factors have been identified that control cell wall thickness (18-19), and specific MYB transcription factors are known to be regulators of secondary cell wall biosynthesis (20-21). Recently, a large transcriptional network that regulates secondary cell wall biosynthesis was elucidated, identifying tens of transcription factors and their role in a complex regulatory network leading to organized secondary wall formation in xylem (22). It was recently

discovered that disruption of MEDIATOR5a/5b can suppress the growth defects of Arabidopsis *ref8*, a mutant defective in lignin biosynthesis (23).

The mediator transcriptional co-activator complex has been found to be a crucial component in promoting eukaryotic transcription as it links transcription factor binding at promoters with the activity of RNA polymerase II (Pol II) (24). Mediator is a multi-subunit protein complex comprising between 25 to 34 subunits depending on the species (25-26) and plays a role in the transcription of both constitutively expressed and inducible genes (27). Mediator has been described as being organized into four sub modules; the head, middle, tail and kinase domains (28). The tail submodule is thought to associate directly with transcriptional activators and repressors and the head with Pol II (24). The Arabidopsis mediator complex was purified (29), and in combination with subsequent bioinformatic analysis (26), thirty-four subunits were identified, a number of these being specific to plants (30). In Arabidopsis, roles for Mediator subunits have been demonstrated in the transcriptional response to a number of biotic (31-33) and abiotic stress conditions (34-35) as well as in plant development (36-37).

In order to better understand the role of *COBRA* in cellulose synthesis, we identified six independent suppressors of the *cob-6* allele, named *MONGOOSE1 to 6*. The *mongoose1* (*mon1*) mutation mapped to the *MEDIATOR16* (*SFR6/MED16*) locus. Analysis of the effects of mutations in *MED16* on transcription identified two pectin methylesterase inhibitors (PMEI) that are regulated by MED16. Overexpression of these PMEIs causes partial suppression of *cobra*, suggesting that pectin esterification is a significant factor in cell wall integrity.

Results

Isolation of *mongoose* Mutations

In an effort to understand the function of COBRA, we carried out a suppressor screen for restoration of root growth in plants homozygous for a *cobra* mutation. Since null mutations of *COBRA* are virtually sterile (11), we performed the screen using *cob-6*, a weak T-DNA allele that produces approximately 10% of functional transcripts (38). Approximately 100,000 seeds of a *cob-6* line were mutagenized with ethyl methanesulfonate (EMS) and seedlings were screened in the M2 generation. Six recessive *cob-6* suppressors, *mongoose1-6* (*mon1-6*), were identified (Fig. 1). Allelism tests revealed that the *mon* mutations represent six genes (Fig. S1). The *cobra* mutants are sensitive to increasing concentrations of sucrose (11) and all six suppressors restore normal growth of *cob-6* on high sucrose concentrations as well as normal hypocotyl elongation in dark grown seedlings (Fig. 1).

Previously described suppressors of the *cob-6* mutation have been reported to act by increasing the transcript levels of *COBRA* (39). In contrast, in all six *mon* lines *COBRA* transcript levels were similar to those in *cob-6* (Fig. S1), implying that suppression in these lines is not due to increased accumulation of functional *COBRA* transcripts. We also tested *theseus1* which was found to suppress CESA6 mutant, however *theseus1 failed to suppress cob-6* (Fig S9).

Cellulose Characterization of *mon1 cob-6*

In addition to the growth phenotype, we assessed whether the cellulose defects caused by *cob-6* were suppressed by *mon-1*. We analyzed the cellulose macrostructure and amounts in a line homozygous for *mon1* and *cob-6* (Fig. 2). Cellulose macrostructure was visualized using S4B staining (13). In *cob-6*, defects in cellulose macrostructure can be seen as early as in the division zone, at which point a fine network of thin fibrils can be seen in wild type. In *cob-6* the network appears more diffuse than in wild type, and in addition there are patches of bright staining in *cob-6* that are rarely observed in wild type. In *mon1 cob-6* the staining looks similar to wild type, however not as a define pattern as in wilde type. In mature wild type root cells, cellulose fibrils can be clearly seen. The staining in *cob-6* displays a higher variability between cells, with some cells exhibiting diagonal fibrils and some cells lacking stain completely. In *mon1 cob-6*, S4B staining of elongated cells in the root showed that the cellulose macro structure was

similar to wild type (Fig. 2A). Quantitative measurements of cellulose (Table 1) showed that there is an almost 50% reduction of cellulose in *cob-6*. The *mon1 cob-6* lines showed a significant increase of cellulose levels compared to *cob-6*, albeit still below that of wild type (Table 1). The *mon1* mutation also reversed changes in other polysaccharides in the *cob-6* mutant, as indicated by changes in cell wall sugar composition of the *mon 1 cob-6* line (Table 1).

Further analysis of the molecular structure of *mon1 cob-6* cell walls compared to *cob-6* and wild type, were obtained using Magic-angle-spinning (MAS) solid-state NMR (ssNMR) spectroscopy (Fig. 2C). Our previous ssNMR studies yielded important structural information about the composition and crystallinity of *cob-6* primary cell walls (12). Therefore, we applied quantitative ^{13}C ssNMR by direct polarization experiments using a long recycle delay. As previously shown, there were clear differences between wild type and *cob-6* revealed in the 1D spectrum due to a significant reduction in cellulose and relative increase in pectin and glycoprotein. However, the 1D ^{13}C spectrum of *mon1 cob-6* resembles the wild-type spectrum, indicating a significant recovery of cellulose and decrease in pectin and glycoprotein. Furthermore, the ratio between the intensity of the interior C4 peak (iC4) and surface C4 peak (sC4) of cellulose were measured and while *cob-6* shows 15% lower crystallinity relative to wild type, *mon1 cob-6* shows no difference relative to wild type (Fig. 2D). These microspectroscopy results correlate with the cell wall analysis results (Table 1) and support the conclusion that suppression of *cob-6* by *mon1* involves restoration of cell wall composition and structure.

Mapping of *mon1* to MED16/SFR6

We used bulk segregents approch with genomic DNA sequencing to identify the *mon1* mutation (40). Two hundred segregants from a *mon1 cob-6* line backcrossed to *cob-6* were pooled for whole genome sequencing. The analysis showed that the causative mutation was located on the upper arm of chromsome four (Fig. S2). In the region with SNP frequencies over 80%, there were twenty six mutations in genes, but only five were missense mutations. One of the five candidate SNPs was a C to T mutation at position 5679 in AT4G04920, which leads to a serine-to-phenylalanine substitution at position 889 (Fig. 3A).

To test whether this was the causative mutation we crossed *cob-6* with a previously characterized TDNA mutation in AT4G04920, *sfr6-3* (*sensitive to freezing6*). The *sfr6-3 cob-6* seedlings exhibited normal growth under light (Fig. 3B) and dark (Fig. 3C) conditions. Cellulose analysis (Fig. 3D) revealed that *sfr6-3 cob-6* cellulose levels were similar to that in *mon1 cob-6* - significantly higher than *cob-6*, but lower than wild type. *COBRA* transcript levels in *sfr6-3 cob-6* were the same as in *cob-6* and in *mon1 cob-6* (Fig. S3). These results demonstrate that the suppression in *mon1 cob-6* is due to a mutation in AT4G04920.

SFR6 was originally identified in a screen for plants that are sensitive to freezing after cold acclimation (41). *sfr6-1* was mapped to AT4G04920 and additional T-DNA alleles, *sfr6-2* and *sfr6-3,* were characterized (42). We performed freezing experiments for the different lines using acclimated and non-acclimated plants (Fig. S4). *sfr6-3* was sensitive to freezing despite cold acclimation, as expected. With no cold acclimation, wild type was sensitive to freezing, as well as *sfr6-3*, *mon1 cob-6* and *sfr6-3 cob-6*. However, *cob-6* was resistant to freezing, even when the plants were not acclimated (Figure S4). We hypothesized that this might be due to altered expression of genes that respond to the cell wall damage of *cob-6* that are also involved in cold acclimation. To check this, we analyzed the expression of *CBF1*, a transcription factor that is known to be upregulated during cold acclimation (43). The results confirmed that in *cob-6* plants, *CBF1* is upregulated without cold acclimation (Fig. S4).

Characterization of MED16 Mutations as Suppressors of Cellulose-Deficiency

Seedlings of *sfr6-3* are larger than wild type (Fig. 3), but there is no other obvious phenotype under normal growth conditions. However, *sfr6* mutants were shown to be hyper-sensitive to freezing, as well as to osmotic stress (44). To test the response of *sfr6-3* to perturbations in cellulose synthesis, we performed cellulose biosynthesis inhibitor assays (Fig. 4). Multiple cellulose biosynthesis inhibitors are known, with different effects on the cellulose synthase complex (45). 2,6-Dichlorobenzonitrile (DCB) causes reduction of the cellulose synthase complex velocity, whereas isoxaben, which is thought to specifically target the cellulose synthase complex, causes depletion of the cellulose synthase complex from the

plasma membrane (46). Indaziflam was recently characterized to cause reduction in mobility of the cellulose synthase complex (47).

To test the response to the different cellulose biosynthesis inhibitors, seedlings were grown on ½MS plates with increasing concentrations of the drugs for 7 days (Fig. 4). To avoid bias by the various root phenotypes, for each line we plotted the relative root length compared to growth with no inhibitors (Fig. 4, Y axis). For each line, fifty seedlings were measured and growth inhibition (GI50) was calculated (Fig. 4). The results are similar for all three inhibitors (Fig. 4). *cobra* is hyper-sensitive to all of the inhibitors, although the response to isoxaben is more dramatic compared to DCB and indaziflam. In contrast, *sfr6-3* is significantly more resistant than wild type to all of the inhibitors. Although *mon1 cob-6* and *sfr6-3 cob-6* exhibit normal root length under control conditions or even when grown with 2% sucrose, which enhances the *cobra* phenotype (Fig. 1), they were found to be more sensitive than wild type to the inhibitors, although still significantly more resistant than *cob-6*. The results in Fig. 4 demonstrate that the mutation in *MED16* (*sfr6-3*) causes resistance to cellulose synthesis perturbation.

Analysis of the Effect of MED16 on Gene Regulation in *cobra* Background.

SFR6 was identified as *MEDIATOR16* (*MED16*), a component of the MEDIATOR transcriptional co-activator complex (32), and is required for RNA polymerase II recruitment of genes regulated by the CBF transcription factor (35). More generally, *MED16* has been shown to regulate expression of multiple genes associated with a variety of biological functions (35) (32). To identify potential targets of *MED16* that are involved in *cobra* suppression, we performed RNA-seq analysis on seven day old seedlings of wild type, *cob-6*, *sfr6-3* and *sfr6-3 cob-6* (Fig. 5A, file S1). Using a 1.5-fold difference in expression value with $p<0.05$ as the cutoff parameter. we identified 277 misregulated genes in *cob-6* (180 ↑, 97 ↓), 302 in *sfr6-3* (29 ↑, 273 ↓) and 677 in *sfr6-3 cob6* (201 ↑, 476 ↓) (Fig. 5A). To have a broad look at the misregulated genes in the three mutants we analyzed the data based on GO annotation (Fig. S5). The biggest difference was found to be in the signal transduction and DNA dependent

transcription classes (Fig. S5), where as expected, there is a larger portion of misregulated genes in these classes for *sfr6-3* and *sfr6-3 cob-6*.

To learn more about the suppression mechanism, we focused on the comparison between *cob-6* to *sfr6-3 cob-6*. First, there are one hundred and forty-eight genes that are misregulated in *cob-6* and are not misregulated in *sfr6-3 cob-6*. It is difficult to evliuate the contribution of these genes (File S1) to *cob-6* phenotype, as genes in this list are spread across cellular loclization and function. We mainlly looked for genes that are misexpressed in *sfr6-3 cob-6* compare to *cob-6* single mutant (FigS5, file S1). To identify potential targets for further analysis we raised the cutoff to two-fold , keeping $P<0.05$). The highest 20 misexpressed genes (10 highest and 10 loest) where either unknown genes or genes with no obious conection to cell wall biosynthesis. We decided to focus on cell wall related genes and found 48 cell wall related genes that are differentially expressed two-fold or greater between *cob-6* and *sfr6-3 cob-6* (14 ↑, 34↓). The largest sub-group within this list were eleven genes involved in the modification of pectin. Our previous in-depth characterization of *cob-6* cell walls revealed that after the reduction in cellulose, the pectin fraction was the most dramatically altered (12), so we focused additional studies on this group.

The Role of MED16 in Pectin Esterification

Pectin is deposited in the apoplast in a highly esterified form, and esterification level decreases during development. Non-esterfied pectin can form calcium bridges that affect its rigidity (48). The degree of pectin esterification was decreased in *cob-6* compared to wild type (Fig. 5B), as reported previously (12). However, the degree of esterification in *cob-6 mon1* or *cob-6 srf6-3* was similar to wild type. This suggests that the suppression mechanism involves the restoration of the pectin esterification, at least in part.

We identified eleven misregulated pectin related genes in *sfr6-3 cob-6* compared to *cob-6*: four pectin lyase-like, two pectin methylesterase and five pectin methylesterase inhibitors

(PMEI). We focused on the two most highly misexpressed PMEIs, AT3G17130 (*PMEI8*) and AT1G62770 (*PMEI9*).

PMEIs can bind to PMEs and inhibit their activity, and have been shown to participate in growth control (49). *PMEI8* is expressed at relatively low levels during development, while *PMEI9* expression is higher in seedlings compared to the rest of the developmental stages (based on expression profile from Genevestigator). We tested the expression of both *PMEI8* and *PMEI9* in the different lines using qRT-PCR (Fig. 5C). Consistent with the RNA-seq data, both *PMEI8* and *PMEI9* were upregulated in *mon1 cob-6* and *sfr6-3 cob-6* compared with wild type (Fig. 5A), the *PMEI9* increase being more striking. *PMEI8* and *PMEI9* expression was slightly reduced in *cob-6* single mutants, and slightly higher in *sfr6-3*, but to a lesser extent. The differences in expression between *sfr6-3* and *mon1 cob-6* suggested that *PMEI8* and *PMEI9* expression is exaggerated when there are cell wall defects. To test this, we analyzed *PMEI8* and *PMEI9* expression in *sfr6-3* after treatment with isoxaben. The results (Fig. S7) showed that indeed, *PMEI8* and *PMEI9* are upregulated significantly when *sfr6-3* seedlings are treated with isoxaben, supporting the idea that regulation of *PMEI8* by *sfr6-3* is affected by an additional stress. To directly test the effect of these two PMEIs on the *cob-6* phenotype, we expressed the genes under control of the 35S promoter in the *cob-6* background (Fig. 5D). The results demonstrate that overexpression of *PMEI8* or *PMEI9* causes partial suppression of the *cob-6* phenotype.

Discussion

Isolation of *cobra* Suppressors

The phenotype of *cobra* mutants includes reduced growth and swollen organs that appear to result from defects in cellulose synthesis and deposition (11-12). Suppression of the swollen root phenotype, but not the root elongation defect, of a *cobra* mutant was observed in the *IAA-Alanine Resistant 4* (*iar4)* mutant (50). The mechanism was suggested to be related to the role of auxin in regulating cell wall loosening (50). Another cellulose deficient mutant, *procuste*, was suppressed by mutation in a receptor-like-kinase, *theseus1* (51).

However, *theseus1* does not suppress *cobra* (Fig. S9), suggesting that not all cellulose deficiencies are equal.

The relatively large number of *cobra* suppressors reported here raises the possibility that some or all of the *mon* mutations may be in a common pathway for what is obviously a dispensable function under laboratory conditions. Additional research will be required to characterize the functions of the other *MONGOOSE* genes, and to identify any other mutations that can be recovered by expanding the screen. Whatever the case, identification of *MED16* as a *cob-6* suppressor contributes to our knowledge of the transcriptional regulation of genes involved in cell wall biosynthesis or remodeling.

Mediator16 as a *cobra* Suppressor

Mediator subunits, particularly those comprising the tail submodule, interact with transcription factors to control gene expression (52). However, no MED16-interacting transcription factors from plants have been identified to date. Lines carrying a mutation in *MED16* (EMS lines *sfr6-1*, T-DNA insertion lines *sfr6-2*, *sfr6-3*, and *yid1*) do not exhibit major phenotypic changes under normal conditions. *sfr6* mutants are slightly larger than their wild-type counterparts at the seedling stage (Fig. 3) (42), and exhibit pale, chlorotic leaves (42) (53), which was recently found to be attributable to iron deficiency (53). The largest phenotypic differences observed between *med16* mutants and wild-type plants are seen under abiotic and biotic stress conditions; *med16* mutants are sensitive to freezing, osmotic stress, pathogen attack and iron deficiency (42, 44, 53). In correlation, our RNA-seq data shows that in *sfr6-3* three hundred and two genes are misregulated compare to wild type, and six hundred and seventy seven genes are misregulated in *sfr6-3 cob-6* double mutant, emphasis the effect of an additional stress on sfr6-3 mutants. Our result that *sfr6-3 cob-6* plants are not sensitive to freezing suggests that med16 is not essential for freezing tolerance (Fig. S4). We found *sfr6-3* to be resistance to cellulose biosynthesis inhibitors, and it will be interesting to examine the behavior of the CESA particles in this mutant. Based on expression data from Genevestigator (54), *MED16* expression does not change dramatically under perturbation conditions. Due to its

position in the yeast mediator complex, where Sin4 (a yeast MED16 homolog) links the so-called "triad" of tail subunits to the rest of the complex (55), it has been suggested that some of the phenotypes associated with loss of MED16 in Arabidopsis may be attributable to loss of other tail subunits that require MED16 to tether them to the complex (35).

Transcriptome analysis has been carried out previously for *sfr6* using microarrays on 7-8 day old seedlings (35). These studies had implicated *MED16* as a factor in the transcriptional regulation of some aspects of cell wall biosynthesis or remodeling. Here we performed RNA-seq analysis on *sfr6-3* as well as *sfr6-3 cob-6*. Three hundred and two genes are misregulated in *sfr6-3*, while six hundred and seventy seven genes are misregulated in *sfr6-3 cob-6*. One hundred and forty-eight genes that are misregulated in *cob-6* are not misregulated in *sfr6-3 cob-6*. It is not obvious whether this is a cause or an effect of the suppression of *cob-6* by *sfr6-3*. It is possible that the elevation in cellulose levels in *mon1 cob-6* cause suppression of *cob-6* phenotype. On the one hand it is possible that the *cob-6* mutation triggers a cascade of gene expression changes that cause the phenotypes, and that a phenotypically-important part of that cascade is blocked by the *sfr6-3* mutation. Alternatively, the phenotypes might be caused directly by the loss of COBRA function in *cob-6*, the usual working assumption (12), and the *sfr6-3* mutation suppresses those effects by altering expression of genes that encode compensating functions. Unfortunately, the large number of misregulated genes is a barrier to a simple explanation for the mechanistic basis for the suppression of *cob-6* by mutations in *MED16*. However, the observation that ectopic constitutive expression of two MED16-regulated genes (*PMEI8*, *PMEI9*) causes partial suppression of the *cob-6* phenotype suggests that a significant component of the suppression effect is via pectin modification.

Pectin Esterification and Freezing Tolerance

Both pectin amounts and degree of esterification increase after cold acclimation (56). Therefore, the regulation of pectin content and degree of esterification that is partially mediated by MED16 might contribute to the established role of MED16 in freezing tolerance.

In *cob-6* plants the pectin is highly non-esterified, and the plants are resistant to freezing (Fig. S4). However, *CBF1* is upregulated in *cob-6* even when plants are not cold

acclimated. This fact is likely to be the most significant factor in the freezing tolerance of non-acclimated *cob-6*. Assuming that the primary effect of the *cob-6* mutation is a defect in cellulose synthesis (12), the implication seems to be that altered cell wall structure can induce *CBF1*.

Pectin Esterification and Cellulose Biosynthesis

We have previously shown that the pectin fraction in the *cobra* mutant is highly non-esterified (12). Introduction of *PMEI8* and *PMEI9* under control of the 35S promoter increases the amount of pectin esterification in the *cob-6* mutant to essentially wild type levels and partially suppresses the *cobra* phenotype. This effect runs counter to the notion that increased Ca^{2+}-mediated crosslinking of non-esterified pectin may compensate for a defect in cellulose synthesis by strengthening the cell wall. Thus, it is unclear why increased non-esterified pectin partially suppressed the *cobra* phenotype. One possibility arises from the observation that changes in pectin esterification can trigger brassinosteroid signaling, resulting in cell wall remodeling (57). Perhaps such remodeling compensates for the cell wall defects in *cobra* mutants. Another, highly speculative, possibility is that pectin methylation may affect the binding of pectin to nascent cellulose microfibrils during cellulose synthesis. Pectin has been shown to bind cellulose (58). Perhaps methylated pectin is less disruptive or inhibitory to cellulose crystallization, a process that appears to be defective in the cobra mutants (12), or to some other aspect of cell wall assembly.

Materials and Methods

The materials and methods are available in the Supplementary Information.

Acknowledgments

We thank Trevor Yeats and Tamara Vellosillo for helpful advice and for their comments on the manuscript. We also thank Sam Coradetti and Alex Schultink for their help in analyzing the NGS data. This work was supported by grants from the Energy Biosciences Institute to CRS and DEW

and by the USDA National Institute of Food and Agriculture, Hatch project CA-B-PLB-0077-H**.** NS was the recipient of Postdoctoral Award no. FI-434-2010 from the Binational Agricultural Research and Development Fund. This work used the Vincent J. Coates Genomics Sequencing Laboratory at UC Berkeley, supported by NIH S10 Instrumentation Grants S10RR029668 and S10RR027303.

References

1. Somerville C*, et al.* (2004) Toward a systems approach to understanding plant cell walls. *Science* 306:2206-2211.
2. Wallace IS & Somerville CR (2015) A Blueprint for Cellulose Biosynthesis, Deposition, and Regulation in Plants. *Plant Cell Wall Patterning and Cell Shape*, ed Fukuda H (Wiley Online Library), pp 65-97.
3. McFarlane HE, Doring A, & Persson S (2014) The cell biology of cellulose synthesis. *Annu Rev Plant Biol* 65:69-94.
4. Li S, Bashline L, Lei L, & Gu Y (2014) Cellulose synthesis and its regulation. *Arabidopsis Book* 12:e0169.
5. Kumar M & Turner S (2015) Plant cellulose synthesis: CESA proteins crossing kingdoms. *Phytochemistry* 112:91-99.
6. Fernandes AN*, et al.* (2011) Nanostructure of cellulose microfibrils in spruce wood. *Proc Natl Acad Sci USA* 108:E1195-E1203.
7. Sethaphong L*, et al.* (2013) Tertiary model of a plant cellulose synthase. *Proc Natl Acad Sci U S A* 110:7512-7517.
8. Gu Y*, et al.* (2010) Identification of a cellulose synthase-associated protein required for cellulose biosynthesis. *Proc Natl Acad Sci U S A* 107:12866-12871.
9. Persson S, Wei H, Milne J, Page GP, & Somerville CR (2005) Identification of genes required for cellulose synthesis by regression analysis of public microarray data sets. *Proc Natl Acad Sci U S A* 102:8633-8638.
10. Schindelman G*, et al.* (2001) COBRA encodes a putative GPI-anchored protein, which is polarly localized and necessary for oriented cell expansion in Arabidopsis. *Genes Dev* 15:1115-1127.
11. Roudier F*, et al.* (2005) COBRA, an Arabidopsis extracellular glycosyl-phosphatidyl inositol-anchored protein, specifically controls highly anisotropic expansion through its involvement in cellulose microfibril orientation. *Plant Cell* 17:1749-1763.
12. Sorek N*, et al.* (2014) The Arabidopsis COBRA protein facilitates cellulose crystallization at the plasma membrane. *J Biol Chem* 289:34911-34920.
13. Anderson CT, Carroll A, Akhmetova L, & Somerville C (2010) Real-time imaging of cellulose reorientation during cell wall expansion in Arabidopsis roots. *Plant Physiol* 152:787-796.
14. Whitney SEC, Brigham JE, Darke AH, Reid JSG, & Gidley MJ (1995) In-Vitro Assembly of Cellulose/Xyloglucan Networks - Ultrastructural and Molecular Aspects. *Plant J* 8:491-504.
15. Zykwinska AW, Ralet MC, Garnier CD, & Thibault JF (2005) Evidence for in vitro binding of pectin side chains to cellulose. *Plant Physiol* 139:397-407.
16. Wang T, Zabotina O, & Hong M (2012) Pectin-cellulose interactions in the Arabidopsis primary cell wall from two-dimensional magic-angle-spinning solid-state nuclear magnetic resonance. *Biochemistry* 51:9846-9856.
17. Zhong R & Ye ZH (2007) Regulation of cell wall biosynthesis. *Curr Opin Plant Biol* 10:564-572.
18. Mitsuda N, Seki M, Shinozaki K, & Ohme-Takagi M (2005) The NAC transcription factors NST1 and NST2 of Arabidopsis regulate secondary wall thickenings and are required for anther dehiscence. *Plant Cell* 17:2993-3006.
19. Zhong RQ, Demura T, & Ye ZH (2006) SND1, a NAC domain transcription factor, is a key regulator of secondary wall synthesis in fibers of Arabidopsis. *Plant Cell* 18:3158-3170.
20. Wang SC*, et al.* (2014) Regulation of secondary cell wall biosynthesis by poplar R2R3 MYB transcription factor PtrMYB152 in Arabidopsis. *Scientific Reports* 4:5054.
21. Yang CY*, et al.* (2007) Arabidopsis MYB26/MALE STERILE35 regulates secondary thickening in the endothecium and is essential for anther dehiscence. *Plant Cell* 19:534-548.

22. Taylor-Teeples M*, et al.* (2015) An Arabidopsis gene regulatory network for secondary cell wall synthesis. *Nature* 517:571-575.
23. Bonawitz ND*, et al.* (2014) Disruption of Mediator rescues the stunted growth of a lignin-deficient Arabidopsis mutant. *Nature* 509:376-380.
24. Kornberg RD (2005) Mediator and the mechanism of transcriptional activation. *Trends Biochem Sci* 30:235-239.
25. Bjorklund S & Gustafsson CM (2005) The yeast Mediator complex and its regulation. *Trends Biochem Sci* 30:240-244.
26. Bourbon HM (2008) Comparative genomics supports a deep evolutionary origin for the large, four-module transcriptional mediator complex. *Nucleic Acids Res* 36:3993-4008.
27. Ansari SA, He Q, & Morse RH (2009) Mediator complex association with constitutively transcribed genes in yeast. *Proc Natl Acad Sci U S A* 106:16734-16739.
28. Dotson MR*, et al.* (2000) Structural organization of yeast and mammalian mediator complexes. *Proc Natl Acad Sci U S A* 97:14307-14310.
29. Backstrom S, Elfving N, Nilsson R, Wingsle G, & Bjorklund S (2007) Purification of a plant mediator from Arabidopsis thaliana identifies PFT1 as the Med25 subunit. *Mol Cell* 26:717-729.
30. Mathur S, Vyas S, Kapoor S, & Tyagi AK (2011) The Mediator complex in plants: structure, phylogeny, and expression profiling of representative genes in a dicot (Arabidopsis) and a monocot (rice) during reproduction and abiotic stress. *Plant Physiol* 157:1609-1627.
31. Kidd BN*, et al.* (2009) The mediator complex subunit PFT1 is a key regulator of jasmonate-dependent defense in Arabidopsis. *Plant Cell* 21:2237-2252.
32. Wathugala DL*, et al.* (2012) The Mediator subunit SFR6/MED16 controls defence gene expression mediated by salicylic acid and jasmonate responsive pathways. *New Phytol* 195:217-230.
33. Zhang X, Wang C, Zhang Y, Sun Y, & Mou Z (2012) The Arabidopsis mediator complex subunit16 positively regulates salicylate-mediated systemic acquired resistance and jasmonate/ethylene-induced defense pathways. *Plant Cell* 24:4294-4309.
34. Elfving N*, et al.* (2011) The Arabidopsis thaliana Med25 mediator subunit integrates environmental cues to control plant development. *Proc Natl Acad Sci U S A* 108:8245-8250.
35. Hemsley PA*, et al.* (2014) The Arabidopsis mediator complex subunits MED16, MED14, and MED2 regulate mediator and RNA polymerase II recruitment to CBF-responsive cold-regulated genes. *Plant Cell* 26:465-484.
36. Gillmor CS*, et al.* (2010) The MED12-MED13 module of Mediator regulates the timing of embryo patterning in Arabidopsis. *Development* 137:113-122.
37. Zheng Z, Guan H, Leal F, Grey PH, & Oppenheimer DG (2013) Mediator subunit18 controls flowering time and floral organ identity in Arabidopsis. *PLoS One* 8:e53924.
38. Ko JH, Kim JH, Jayanty SS, Howe GA, & Han KH (2006) Loss of function of COBRA, a determinant of oriented cell expansion, invokes cellular defence responses in Arabidopsis thaliana. *J Exp Bot* 57:2923-2936.
39. Xue W*, et al.* (2012) Paramutation-like interaction of T-DNA loci in Arabidopsis. *PLoS One* 7:e51651.
40. Schneeberger K (2014) Using next-generation sequencing to isolate mutant genes from forward genetic screens. *Nat Rev Genet* 15:662-676.
41. McKown R, Kuroki G, & Warren G (1996) Cold responses of Arabidopsis mutants impaired in freezing tolerance. *J Exp Bot* 47:1919-1925.
42. Knight H*, et al.* (2009) Identification of SFR6, a key component in cold acclimation acting post-translationally on CBF function. *Plant J* 58:97-108.

43. Park S*, et al.* (2015) Regulation of the Arabidopsis CBF regulon by a complex low-temperature regulatory network. *Plant J* 82:193-207.
44. Boyce JM*, et al.* (2003) The sfr6 mutant of Arabidopsis is defective in transcriptional activation via CBF/DREB1 and DREB2 and shows sensitivity to osmotic stress. *Plant J* 34:395-406.
45. Brabham C & Debolt S (2012) Chemical genetics to examine cellulose biosynthesis. *Front Plant Sci* 3:309.
46. Paredez AR, Somerville CR, & Ehrhardt DW (2006) Visualization of cellulose synthase demonstrates functional association with microtubules. *Science* 312:1491-1495.
47. Brabham C*, et al.* (2014) Indaziflam herbicidal action: a potent cellulose biosynthesis inhibitor. *Plant Physiol* 166:1177-1185.
48. Harholt J, Suttangkakul A, & Vibe Scheller H (2010) Biosynthesis of pectin. *Plant Physiol* 153:384-395.
49. Pelletier S*, et al.* (2010) A role for pectin de-methylesterification in a developmentally regulated growth acceleration in dark-grown Arabidopsis hypocotyls. *New Phytol* 188:726-739.
50. Steinwand BJ*, et al.* (2014) Alterations in auxin homeostasis suppress defects in cell wall function. *PLoS One* 9:e98193.
51. Hematy K*, et al.* (2007) A receptor-like kinase mediates the response of Arabidopsis cells to the inhibition of cellulose synthesis. *Curr Biol* 17:922-931.
52. Conaway RC & Conaway JW (2011) Function and regulation of the Mediator complex. *Curr Opin Genet Dev* 21:225-230.
53. Yang Y*, et al.* (2014) The Arabidopsis Mediator subunit MED16 regulates iron homeostasis by associating with EIN3/EIL1 through subunit MED25. *Plant J* 77:838-851.
54. Hruz T*, et al.* (2008) Genevestigator v3: a reference expression database for the meta-analysis of transcriptomes. *Adv Bioinformatics* 2008:420747.
55. Kang JS*, et al.* (2001) The structural and functional organization of the yeast mediator complex. *J Biol Chem* 276:42003-42010.
56. Solecka D, Zebrowski J, & Kacperska A (2008) Are pectins involved in cold acclimation and de-acclimation of winter oil-seed rape plants? *Ann Bot* 101:521-530.
57. Wolf S*, et al.* (2014) A receptor-like protein mediates the response to pectin modification by activating brassinosteroid signaling. *Proc Natl Acad Sci U S A* 111:15261-15266.
58. Dick-Perez M*, et al.* (2011) Structure and interactions of plant cell-wall polysaccharides by two- and three-dimensional magic-angle-spinning solid-state NMR. *Biochemistry* 50:989-1000.

Figure Legends

Figure 1 – Phenotypes of the *mongoose* mutants. All *mon* lines are also homozygous for the *cob-6* mutation.

Figure 2 – Cellulose macrostucture and amount in *mon1 cob-6* mutant. A) Cellulose in root cells stained with S4B. In *cob-6*, staining is reduced and less homogeneous, with some cells exhibiting almost a complete lack of fluorescence. Fibrils that can be detected are not as defined as in wild type, and are not as regularly oriented (upper panel, *cob-6*). In *mon1 cob-6*, fibrils were similar to wild-type, moreso in elongated cells. Scale bars are 15 μm. B) 1D SSNMR analysis. Quantitative ^{13}C DP-MAS ssNMR spectra of wild type, *cob-6* and *mon1 cob-6* cell walls. C) Relative intensities of interior and surface cellulose C4 signals from ^{13}C DP-MAS spectra.

Figure 3 – Properties of MED16 mutants. A) Gene structure of AT4G04920 (*MED16*) showing T-DNA insertion sites and the *mon1* mutation. B) and C) Growth phenotype of seven day light-grown seedlings (B) and five day dark-grown hypocotyls (C) showing suppression of *cob-6* phenotype by *mon1* and *sfr6-3*. D) Cellulose measurement showing suppression of *cob-6* cellulose deficiency.

Figure 4 – Mutation in *MED16* (*sfr6-3*) causes resistance to cellulose biosynthesis inhibitors. Seedling root length of wild type (•), *cob-6* (o), *sfr6-3* (▼), *mon1 cob-6* (Δ) and *sfr6-3 cob-6* (■) grown on ½MS plates with increasing concentrations of the inhibitor for seven days was measured. To avoid bias by the mutant root phenotypes, the root length was compared to the root length with no drug (Y axis – relative root length). The plots present the root lengths relative to the control, and the standard errors (n = 50). The data was fitted using sigmoidal dose-response + hill slope. For statistical analysis, we performed ANOVA coupled TUKEY test on the raw data. Growth inhibition (GI50) shows that *sfr6-3* is significantly more resistant to all of the cellulose biosynthesis inhibitors.

Figure 5 – Increased transcription of pectin methylesterase inhibitors and the restoration of pectin esterification to wild-type levels in *mon1 cob-6* and *sfr6-3 cob-6*. A) Venn diagram for RNA-seq analysis of *cob-6*, *sfr6-3* and *sfr6-3 cob-6*. This diagrm present all genes that are upregulated and downregulated compared to wild type with 1.5 fold change or above. For further analysis, we looked at genes that are misexpressed between *sfr6-3 cob-6* and *cob-6*, and identified 48 cell wall related genes (see file S1). B) Pectin esterification levels in the different lines. Values were normalized to the total amount of galacturonic acid (Fig. S8). C) Steady-state mRNA levels of two pectin methylesterase inhibitor genes AT3G17130 (*PMEI8*) and AT1G62770 (*PMEI9*) in various genotypes. D) *PMEI8* and *PMEI9* were overexpressed in the *cob-6* background. Ten independent lines were analyzed, all demonstrated partial suppression of the *cob-6* phenotype.

Tables

Table 1 Monosaccharide and cellulose analysis. Values are ug per mg of alcohol insoluble residue. Superscripts represents statistical differences of $p < 0.05$ by two-way analysis of variance coupled to Tukey test. The high level og Galactose (Gal) and Arabinose (Ara) in *cob-6* are due to the high level of pectin in the mutant

	WT	*cob-6*	*mon1 cob-6*
Man	6.2 ± 0.2^{A}	7.1 ± 0.2^{B}	6.5 ± 0.1^{A}
Fuc	4.1 ± 0.1^{A}	3.8 ± 0.2^{A}	4.2 ± 0.2^{A}
Ara	19.4 ± 0.6^{A}	37.5 ± 0.8^{B}	21.3 ± 0.3^{C}
Glu	9.8 ± 0.2^{A}	11.1 ± 0.2^{B}	10.0 ± 0.3^{A}
Xyl	20.9 ± 0.5^{A}	21.1 ± 0.4^{A}	20.5 ± 0.7^{A}
Rha	11.1 ± 0.3^{A}	11.4 ± 0.4^{A}	11.1 ± 0.3^{A}
Gal	45.8 ± 2.1^{A}	74.3 ± 4.2^{B}	50.1 ± 3.5^{A}
Cellulose	122 ± 3.2^{A}	65 ± 4.7^{B}	105 ± 2.4^{C}

Figure 1

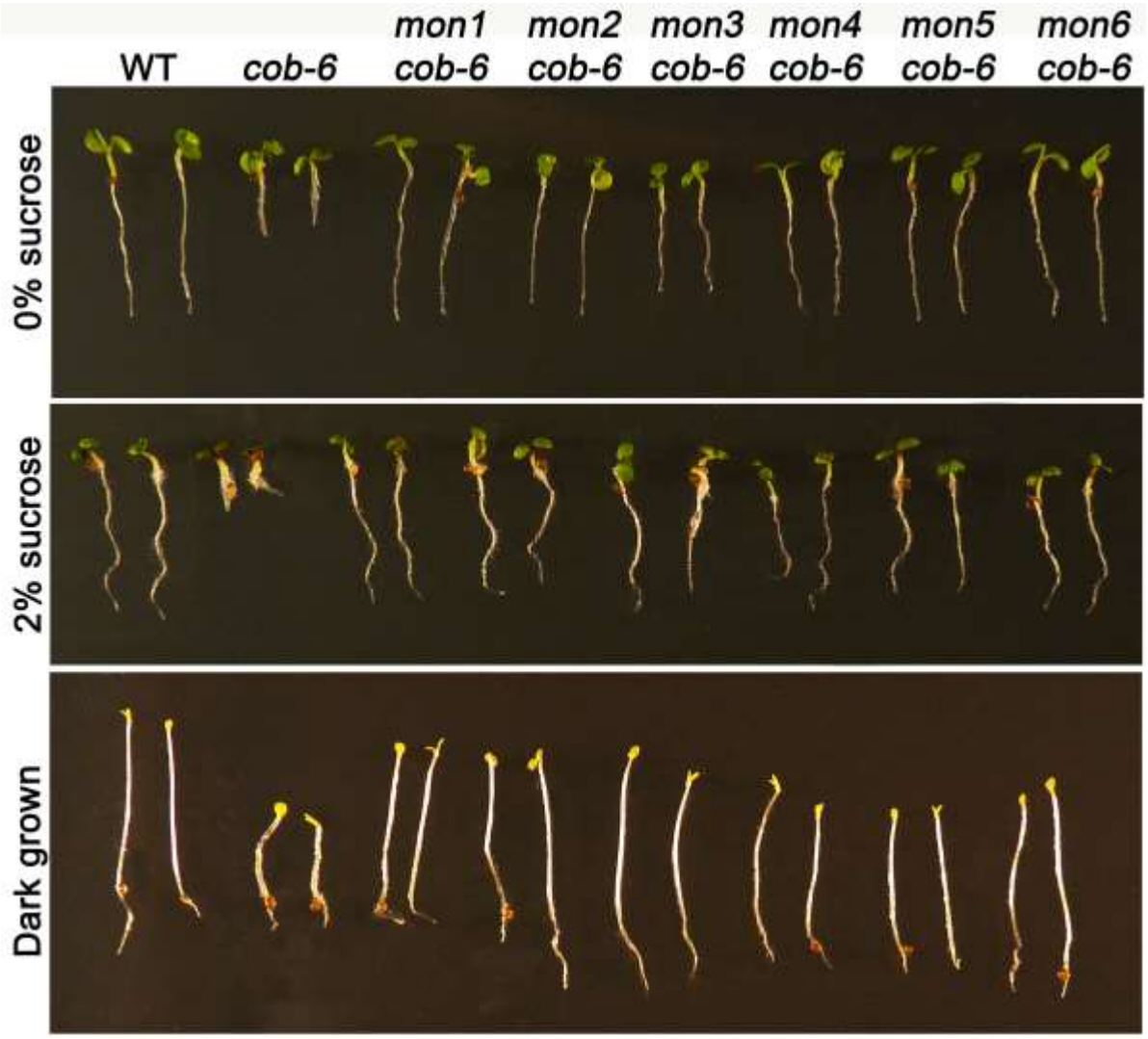
WT
cob-6
mon1 cob-6
mon2 cob-6
mon3 cob-6
mon4 cob-6
mon5 cob-6
mon6 cob-6
0% sucrose
2% sucrose
Dark grown

Figure 2

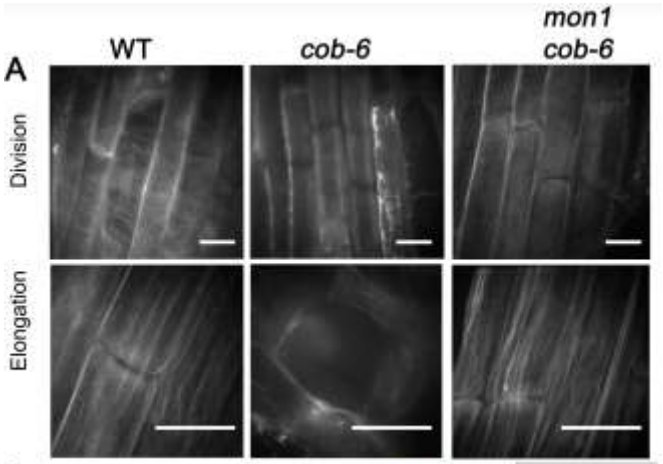

C

Genotype	I(iC4) 88.5-91 ppm	I(sC4) 84-86 ppm	I(iC4)/I(sC4)	Normalized
WT	10.7E9	15.9E9	0.67	1.00
cob-6	5.3E9	9.3E9	0.58	0.85
mon1 cob-6	9.2E9	13.8E9	0.67	1.00

Figure 3


A
AT4G04920 - MED16 (SFR6)
sfr6-2
sfr6-3
mon1
ser→phe
B
WT
cob-6
sfr6-3
mon1 cob-6
sfr6-3 cob-6
C
D
Cellulose (µg/mg AIR)
140
120
100
80
60
40
20
0
A
B
A
C
C
WT
cob-6
sfr6-3
mon1 cob-6
sfr6-3 cob-6

Figure 4

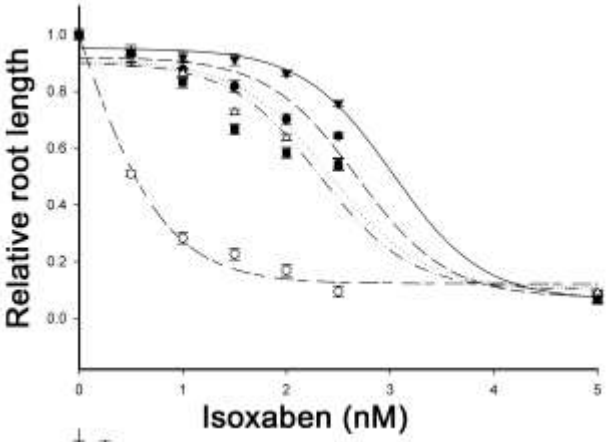

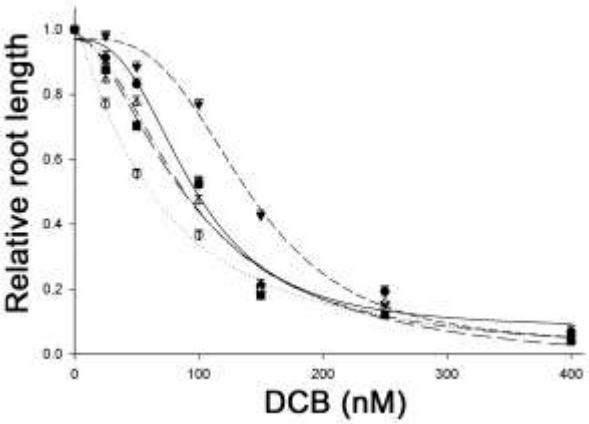

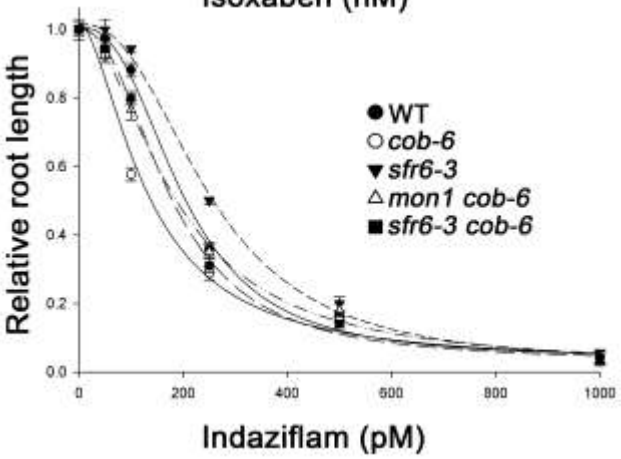

Growth inhibition (GI50)			
Genotype	**Isoxaben (nM)**	**DCB (nM)**	**Indozaflin (pM)**
WT	2.81±0.21^{A}	102±8^{A}	220±10^{A}
cob-6	0.53±0.07^{B}	57±2^{B}	167±7^{B}
sfr6-3	3.11±0.15^{C}	138±8^{C}	274±11^{C}
mon1 cob-6	2.58±0.14^{D}	92±5^{D}	198±9^{D}
sfr6-3 cob-6	2.51±0.12^{D}	88±^{D}	191±7^{D}

Figure 5

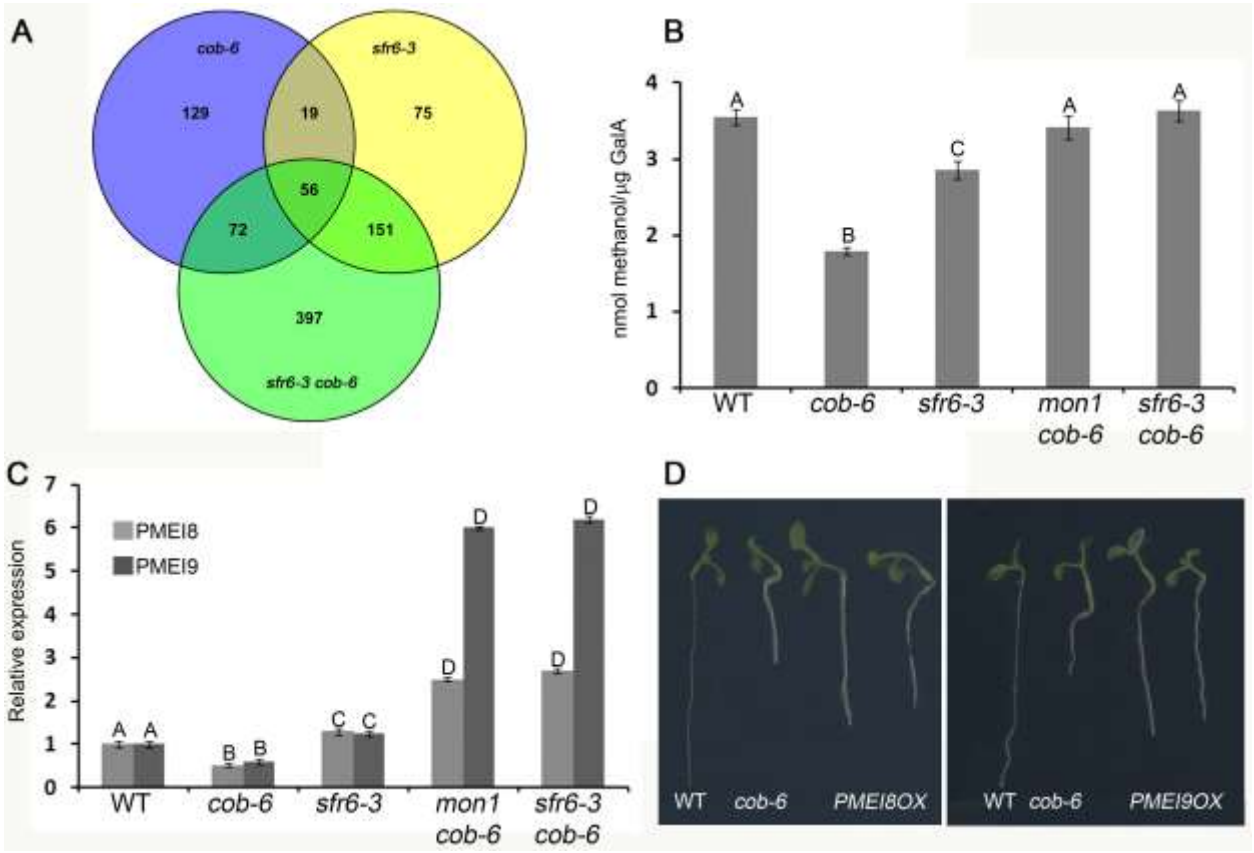
A
cob-6
sfr6-3
129
19
75
56
72
151
397
sfr6-3 cob-6
B
nmol methanol/µg GalA
WT
cob-6
sfr6-3
mon1 cob-6
sfr6-3 cob-6
C
Relative expression
PMEI8
PMEI9
D
WT
cob-6
PMEI8OX
PMEI9OX